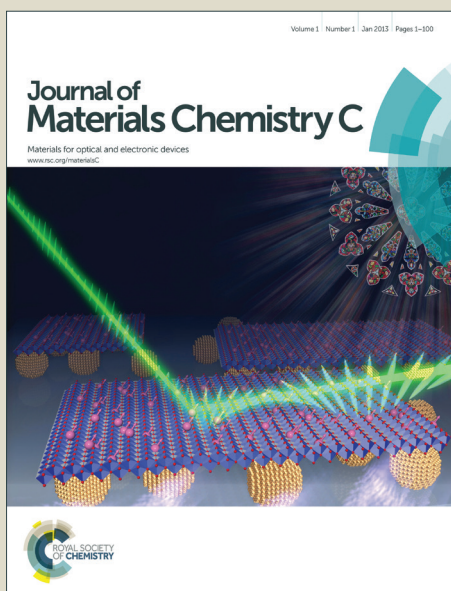


Journal of Materials Chemistry C

Accepted Manuscript



This is an *Accepted Manuscript*, which has been through the Royal Society of Chemistry peer review process and has been accepted for publication.

Accepted Manuscripts are published online shortly after acceptance, before technical editing, formatting and proof reading. Using this free service, authors can make their results available to the community, in citable form, before we publish the edited article. We will replace this *Accepted Manuscript* with the edited and formatted *Advance Article* as soon as it is available.

You can find more information about *Accepted Manuscripts* in the [Information for Authors](#).

Please note that technical editing may introduce minor changes to the text and/or graphics, which may alter content. The journal's standard [Terms & Conditions](#) and the [Ethical guidelines](#) still apply. In no event shall the Royal Society of Chemistry be held responsible for any errors or omissions in this *Accepted Manuscript* or any consequences arising from the use of any information it contains.

A novel warm white emitting phosphor $\text{Ca}_2\text{PO}_4\text{Cl}:\text{Eu}^{2+}, \text{Mn}^{2+}$ for white LEDs

Panlai Li*, Zhijun Wang*, Zhiping Yang, Qinglin Guo

College of Physics Science & Technology, Hebei University, Baoding 071002, China

Abstract: A series of single phase phosphors $\text{Ca}_2\text{PO}_4\text{Cl}:\text{Eu}^{2+}, \text{Mn}^{2+}$ are successfully synthesized by a solid-state method, and their photoluminescence properties are investigated. $\text{Ca}_2\text{PO}_4\text{Cl}:\text{Eu}^{2+}, \text{Mn}^{2+}$ can be excited at wavelength ranging from 250 to 450 nm, which is well matched with ultraviolet light emitting diode. As a result of fine-tuning of emission composition of Eu^{2+} and Mn^{2+} ions, warm white light can be realized by combining the emission of Eu^{2+} and Mn^{2+} in a single host lattice under ultraviolet light excitation. Efficient resonant energy transfer from Eu^{2+} to Mn^{2+} ions is demonstrated to be a dipole-quadrupole mechanism in $\text{Ca}_2\text{PO}_4\text{Cl}$, and the energy transfer efficiency enhances with increasing Mn^{2+} concentration, which is confirmed by luminescence spectra and fluorescence decay times. The energy transfer efficiency and critical distance are also calculated. A warm white light emitting diode is fabricated using the single-phase white emitting phosphor $\text{Ca}_2\text{PO}_4\text{Cl}:0.07\text{Eu}^{2+}, 0.2\text{Mn}^{2+}$ pumped by a 400 nm LED-chip. Our results indicate that CIE chromaticity coordinates and correlated color temperature (CCT) for the white LEDs are (0.3102, 0.3096) and 4296K, respectively. Therefore, $\text{Ca}_2\text{PO}_4\text{Cl}:\text{Eu}^{2+}, \text{Mn}^{2+}$ can serve as potential warm emitting material for white LEDs.

Keywords: Phosphors; Luminescence; White LEDs; $\text{Ca}_2\text{PO}_4\text{Cl}:\text{Eu}^{2+}, \text{Mn}^{2+}$; Energy transfer

1. Introduction

In recent years, white-light-emitting diodes (white LEDs) have been considered to be important solid-state light sources due to their advantages of high brightness, low power consumption, and long duration.¹⁻³ However, white LEDs based on 460 nm blue-chip+YAG: Ce^{3+} phosphor exhibit

*li_panlai@126.com

*wangzj1998@126.com

only a high correlated color temperature (CCT \approx 7750 K) with a poor color rendering index (CRI \approx 70-80) because of the lack of red component.⁴ Recently, white LEDs fabricated using a near ultraviolet (n-UV) LED coupled with red, green and blue phosphors have attracted much attention.⁵ However, the use of multi-phosphors experience different light output degradation rates, leading to the unstable white light, and there is a trade-off in luminous efficiency attributed to reabsorption. Therefore, design of single-phase phosphor pumped by UV chips is of significance for white LEDs because single-phase phosphor has the advantages of excellent color rendering indexes, and the electro-optical design is simple to control different colors in comparison with mixed phosphors.⁶⁻⁸

Upon to now, several single-phase white light emitting phosphors suitable for UV-pumped white LEDs have been reported.⁹⁻¹¹ Some single doped samples, such as Eu³⁺ doped phosphors, can also produce white light,¹² however, most phosphors produce white light by energy transfer from a sensitizer to an activator in the same compound with better color rendering index and lower CCT (about 5000-7500 K), such as Ce³⁺/Eu²⁺, Eu²⁺/Mn²⁺ codoped phosphors, and so on.¹³⁻¹⁵ Moreover, Eu²⁺/Tb³⁺/Mn²⁺ or Ce³⁺/Tb³⁺/Mn²⁺ tri-activated phosphors can also emit white light with the higher color rendering index and lower CCT (approximately 6500 K).¹⁶⁻²⁰ Because warm white light which can be used for indoor illumination, similar to most luminescence lamps, with low CCT (CCT \leq 4500 K or even CCT \leq 3500 K), is more favorable for human sight and more recommended. Obviously, the reported results have seldom to create warm white light which is suitable for indoor application.²¹⁻²³ Hence, it is to be considered as the state of urgency for the development of single-phase warm white emitting phosphor that has lower CCT and excellent luminescence.

As is well known, Eu²⁺ is of great interest for application because d-f emission is partly allowed, resulting in high emission intensity.²⁴ Emission energy shows a strong dependence on crystal field

and covalence, and Eu^{2+} doped phosphors usually have a strong absorption in the region from UV to visible spectra and exhibit broad emission band covering the color from blue to red.²⁵ Generally, the emitting materials consist of activator and host, where the choice of host is considered as the key factor for obtaining efficient emission. Halide-containing oxide-type hosts are good candidates as host structures due to several merits, such as low synthesis temperature, high chemical and physical stability, which exhibit interesting luminescence when doped with Eu^{2+} , such as $\text{Ca}_{12}\text{Al}_{14}\text{O}_{33}\text{Cl}_2$, $\text{Ca}_2\text{Al}_3\text{O}_6\text{F}$, $\text{Ca}_2\text{LiSiO}_4\text{F}$, $\text{La}_6\text{Ba}_4(\text{SiO}_4)_6\text{F}_2$, $\text{Ca}_5(\text{PO}_4)_3\text{F}$, $\text{Sr}_3\text{AlO}_4\text{F}$, $\text{Sr}_3\text{NaLa}(\text{PO}_4)_3\text{F}$, $\text{Sr}_3\text{GdNa}(\text{PO}_4)_3$, $\text{Sr}_5(\text{BO}_3)_3\text{Cl}$, $\text{Ca}_{5.45}\text{Li}_{3.55}(\text{SiO}_4)_3\text{O}_{0.45}\text{F}_{1.55}$, $\text{Ba}_2\text{Ln}(\text{BO}_3)_2\text{Cl}$ (Ln=Y, Gd and Lu), $\text{NaCa}_2\text{LuSi}_2\text{O}_7\text{F}_2$, and so on²⁶⁻⁴⁰. In 1967, Greenblatt et al. reported the X-ray single crystal structure of $\text{Ca}_2\text{PO}_4\text{Cl}$, which crystallized in the orthorhombic system with space group of $\text{pbcm}(57)$ and with four formula units per unit cell ($Z=4$)^{41, 42}. The crystal structure consists of discrete and distorted PO_4^{3-} tetrahedron which are held together primarily by Ca^{2+} ion. Two different crystallographic sites are available for the divalent Ca^{2+} ions, one with site symmetry C_2 and the other with site symmetry C_s . In both sites of the Ca^{2+} is coordinated by six oxide ions and two chloride ion. For the larger C_s site, the average Ca-O distance is about 0.250 nm and the average Ca-Cl distance is 0.289 nm. For the smaller C_2 site, these distances are 0.246 nm and 0.281 nm, respectively^{41, 42}. In the 1990s, Blasse et al. investigated the luminescence and thermoluminescence properties of Eu^{2+} in $\text{Ca}_2\text{PO}_4\text{Cl}$ ⁴³. Chen et al. presented the external quantum efficiency is 61% under 400 nm radiation excitation⁴⁴. Guo et al. studied the synthesization conditions of $\text{Ca}_2\text{PO}_4\text{Cl}:\text{Eu}^{2+}$ ⁴⁵. Based on the effective ionic radii (r) of cations with different coordination numbers (CN)⁴⁴, the ionic radius of Eu^{2+} (for CN=8, $r=0.125$ nm) is close to that of Ca^{2+} (for CN=8, $r=0.112$ nm). Since the four-coordinated P^{5+} ($r=0.017$ nm) site is too small for Eu^{2+} to occupy, the Eu^{2+} is supposed to occupy the Ca^{2+} sites due to size considerations. The

transition metal ion Mn^{2+} can exhibit a broad emission band in the visible range owing to the d-d transition, but it is forbidden and difficult to pump. Because Eu^{2+} ion can act as a good sensitizer transferring a part of its energy to activator ions.¹⁴⁻¹⁶ Therefore, as a promising sensitizer for Mn^{2+} ions, Eu^{2+} can be used to improve the emission intensity of Mn^{2+} in many hosts as mentioned.¹⁴⁻¹⁶ Nevertheless, little attention in literature has been drawn towards luminescence of $\text{Ca}_2\text{PO}_4\text{Cl}:\text{Eu}^{2+}, \text{Mn}^{2+}$, which may have application in white LEDs. Therefore, in the present work, luminescence and energy transfer of $\text{Ca}_2\text{PO}_4\text{Cl}:\text{Eu}^{2+}, \text{Mn}^{2+}$ are explored, and warm white emitting phosphor, with low CCT, is achieved by varying the relative doping content of Eu^{2+} and Mn^{2+} .

2. Experimental

2.1. Sample preparation

A series of $\text{Ca}_{2-x-y}\text{PO}_4\text{Cl}:\text{xEu}^{2+}, \text{yMn}^{2+}$ (x, y molar concentration) samples are synthesized by a high temperature solid-state method. The initial materials, including CaCO_3 (A.R.), $\text{CaCl}_2 \cdot 6\text{H}_2\text{O}$ (A.R.), $\text{NH}_4\text{H}_2\text{PO}_4$ (A.R.), MnCO_3 (A.R.) and Eu_2O_3 (99.99%), are weighed in stoichiometric proportion, thoroughly mixed and ground by an agate mortar and pestle for more than 30 min till they are uniformly distributed. The obtained mixtures are heated at 1000 °C for 2 h in the presence of reducing atmosphere (5% H_2 /95% N_2), and then are naturally cooled to room temperature. In order to measure the characteristics of samples, the samples are ground into powder. White LEDs are fabricated by integrating a mixture of transparent silicone resin and $\text{Ca}_2\text{PO}_4\text{Cl}:\text{Eu}^{2+}, \text{Mn}^{2+}$ on a 400 nm LED chip.

2.2. Materials characterization

Phase formation of $\text{Ca}_{2-x-y}\text{PO}_4\text{Cl}:\text{xEu}^{2+}, \text{yMn}^{2+}$ phosphors is carefully checked by powder X-ray diffraction (XRD) analysis (Bruker AXS D8 advanced automatic diffractometer (Bruker Co.,

German)), with Ni-filtered Cu K α 1 radiation ($\lambda=0.15405$ nm) operating at 40 kV and 40 mA, and a scan rate of 0.02°/s is applied to record the patterns in the 2θ range from 10° to 70°.

Room-temperature photoluminescence spectra and luminescence decay curves are detected by a FLS920 fluorescence spectrometer. The scanning wavelength range from 200 to 700 nm, a spectral resolution of 0.2 nm, and the exciting source is a 450 W Xe lamp. The scanning time range from 0 to 5000 ns, a time resolution is 10 ns, and the exciting source is a EPL 375-picosecond pulsed diode laser. Quantum efficiency is analyzed with a photoluminescence quantum efficiency measurement system (C9920-02, Hamamatsu Photonics, Shizuoka) containing a 150 W xenon lamp. The above measurements are carried out at room temperature. High-temperature photoluminescence spectra are detected by a fluorescence spectrophotometer (Hitachi F-4600) with a TAP-02 high temperature control system, the scanning wavelength range from 400 to 700 nm, a spectral resolution of 0.2 nm, and the exciting source is a 450 W Xe lamp.

3. Results and discussion

3.1. Phase formation

XRD patterns of Ca₂PO₄Cl:Eu²⁺, Ca₂PO₄Cl:Mn²⁺, and Ca₂PO₄Cl:Eu²⁺, Mn²⁺ are measured and a similar diffraction patterns are observed for each sample. As a representative, Fig.1 shows the XRD patterns of Ca₂PO₄Cl:0.07Eu²⁺, Ca₂PO₄Cl:0.4Mn²⁺, Ca₂PO₄Cl:0.07Eu²⁺, 0.2Mn²⁺. When compared the diffraction data with the standard JCPDS card (No.19-0247), and there is no difference between the doped impurity Ca₂PO₄Cl and Ca₂PO₄Cl. The uniform diffraction patterns indicate that the phase formation of Ca₂PO₄Cl is not influenced by a little amounts of Eu²⁺, Mn²⁺, or Eu²⁺/Mn²⁺. However, as shown in Fig.1, with the larger quantity of impurity, such as 0.07Eu²⁺, the XRD pattern peaks slightly shift to the smaller angles (for Mn²⁺ doped Ca₂PO₄Cl, the XRD pattern peaks slightly shift

to the bigger angles). According to Vegard's law, the ionic size of Eu^{2+} (Mn^{2+}) ion is bigger (smaller) than that of Ca^{2+} ion, so it is reasonable. $\text{Ca}_2\text{PO}_4\text{Cl}$ which crystallizes in the orthorhombic system with space group of $\text{pbcm}(57)$ and with four formula units per unit cell ($N=4$), and the dimensions of unit cell are $a=0.6185$ nm, $b=0.6983$ nm and $c=1.082$ nm.

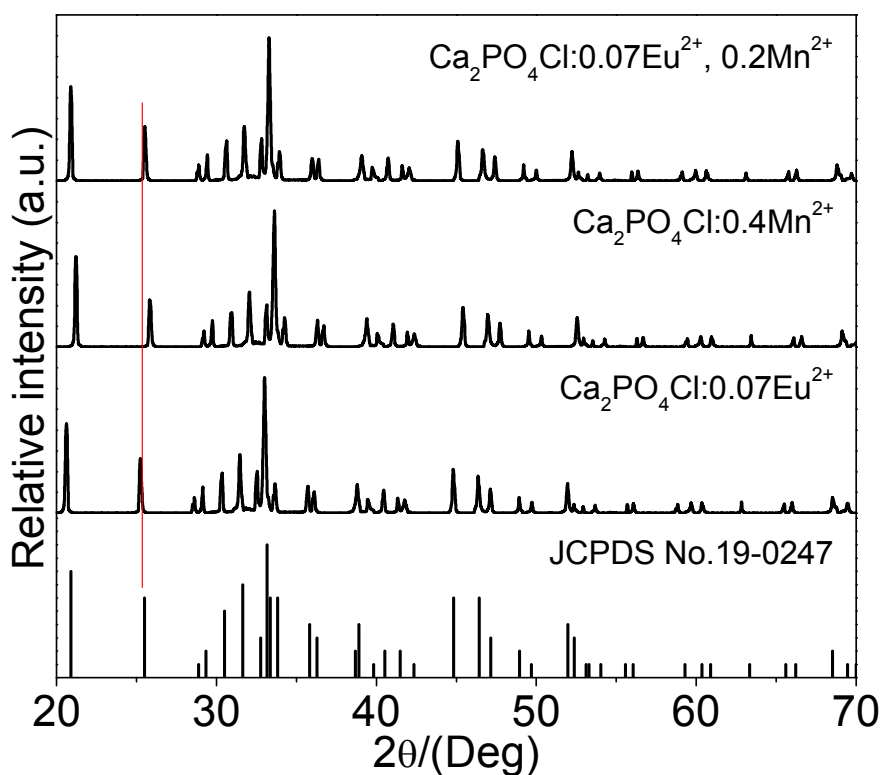


Fig. 1. XRD patterns of $\text{Ca}_2\text{PO}_4\text{Cl}:0.07\text{Eu}^{2+}$, $\text{Ca}_2\text{PO}_4\text{Cl}:0.4\text{Mn}^{2+}$ and $\text{Ca}_2\text{PO}_4\text{Cl}:0.07\text{Eu}^{2+}, 0.2\text{Mn}^{2+}$.

Standard data of $\text{Ca}_2\text{PO}_4\text{Cl}$ (JCPDS No. 19-0247) is shown as reference.

3.2. Luminescent properties of Eu^{2+} and Mn^{2+} in $\text{Ca}_2\text{PO}_4\text{Cl}$

Fig. 2a shows $\text{Ca}_2\text{PO}_4\text{Cl}:0.07\text{Eu}^{2+}$ has a broad emission band under 370 nm radiation excitation, and the peak locates at 450 nm which is typically attributed to $4f^65d^1 \rightarrow 4f^7$ electronic dipole allowed transition of Eu^{2+} ion. Because, two different crystallographic sites are available for the divalent Ca^{2+} ions, one with site symmetry C_2 and the other with site symmetry C_s . Therefore, Eu^{2+} ions may occupy two different Ca^{2+} sites.⁴⁴ Excitation spectrum mainly consists of unresolved band due to the

$4f^7 \rightarrow 4f^6 5d^1$ transition of Eu^{2+} ion. When Eu^{2+} ions occupy the lattice sites with C_2 or C_s symmetry in $\text{Ca}_2\text{PO}_4\text{Cl}$, the fivefold degeneracy of $5d$ levels is expected in excitation spectrum. Nevertheless, the dominating bands in excitation spectrum is difficult to resolve because of serious overlap between $5d$ levels. The broad excitation band is ascribed to the high covalency of $\text{Ca}_{\text{Eu}}\text{-Cl}$ bonding and large crystal-field splitting. Inset of Fig.2a shows the emission spectra of $\text{Ca}_2\text{PO}_4\text{Cl}:\text{xEu}^{2+}$ with different Eu^{2+} concentration. The spectral distribution has the same shape with different Eu^{2+} concentration. However, the emission intensity is influenced by Eu^{2+} concentration, and the optimal concentration is observed to be at $\text{x}=0.07$.

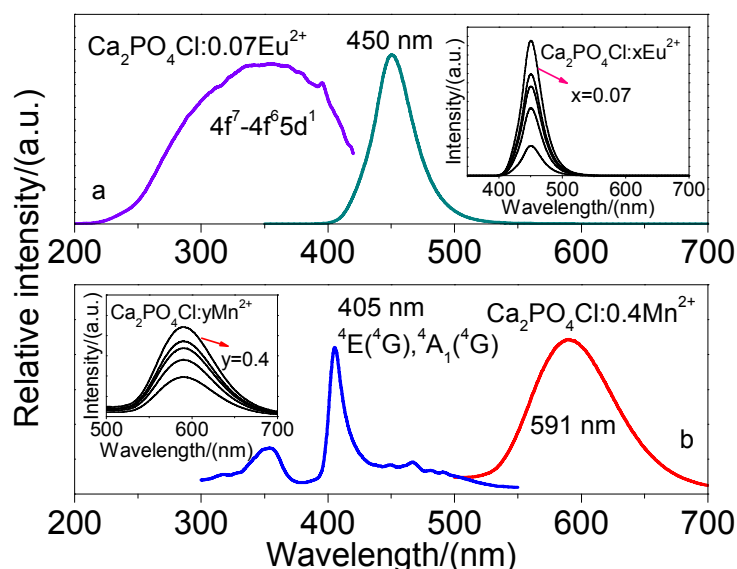


Fig.2. Emission and excitation spectra of (a) $\text{Ca}_2\text{PO}_4\text{Cl}:\text{0.07Eu}^{2+}$ ($\lambda_{\text{ex}}=370$ nm) and (b) $\text{Ca}_2\text{PO}_4\text{Cl}:\text{0.4Mn}^{2+}$ ($\lambda_{\text{ex}}=405$ nm).

Inset: (a) emission spectra of $\text{Ca}_2\text{PO}_4\text{Cl}:\text{xEu}^{2+}$ ($\lambda_{\text{ex}}=370$ nm) with different Eu^{2+} concentration (x);

(b) emission spectra of $\text{Ca}_2\text{PO}_4\text{Cl}:\text{yMn}^{2+}$ ($\lambda_{\text{ex}}=405$ nm) with different Mn^{2+} concentration (y).

Fig.2b presents $\text{Ca}_2\text{PO}_4\text{Cl}:\text{0.4Mn}^{2+}$ has a broad band orange-red emission around 591 nm ascribing to spin-forbidden ${}^4\text{T}_1({}^4\text{G})\text{-}{}^6\text{A}_1({}^6\text{S})$ transition of Mn^{2+} ion. Excitation spectrum of $\text{Ca}_2\text{PO}_4\text{Cl}:\text{Mn}^{2+}$ shows several bands, and the 405 nm strongest excitation corresponds to the transitions from ${}^6\text{A}_1({}^6\text{S})$ ground state to excited states [${}^4\text{E}({}^4\text{G}), {}^4\text{A}_1({}^4\text{G})$].¹⁴⁻¹⁶ With different Mn^{2+}

concentration (y), emission spectra of $\text{Ca}_2\text{PO}_4\text{Cl}:y\text{Mn}^{2+}$ are shown in the inset of Fig.2(b), and the emission intensities primarily enhance with increasing Mn^{2+} concentration, and reach a maximum value at 0.4 Mn^{2+} , then decrease because of concentration quenching.

3.3. Luminescent properties and energy transfer of $\text{Eu}^{2+} \rightarrow \text{Mn}^{2+}$ in $\text{Ca}_2\text{PO}_4\text{Cl}$

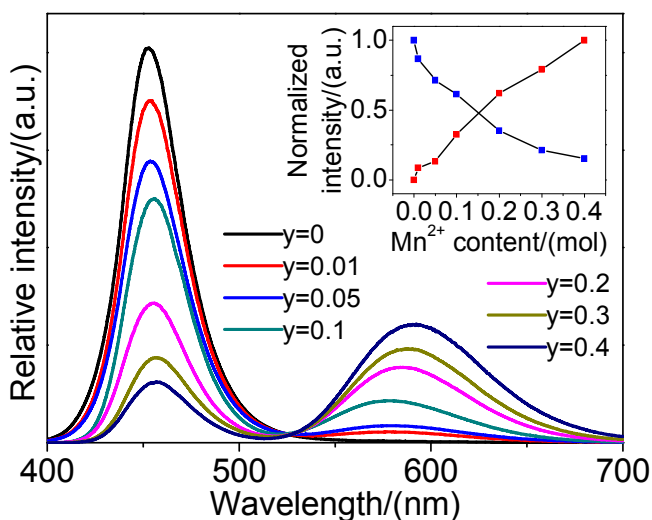


Fig.3. Emission spectra of $\text{Ca}_2\text{PO}_4\text{Cl}:0.07\text{Eu}^{2+}, y\text{Mn}^{2+}$ ($\lambda_{\text{ex}}=370 \text{ nm}$).

Inset: normalized intensity of Eu^{2+} and Mn^{2+} as function of Mn^{2+} concentration ($\lambda_{\text{ex}}=370 \text{ nm}$).

As shown in Fig.2, we can see an obvious spectral-overlap between emission spectrum of Eu^{2+} and excitation spectrum of Mn^{2+} , indicating the possibility of energy transfer from Eu^{2+} to Mn^{2+} in $\text{Ca}_2\text{PO}_4\text{Cl}$. In order to investigate luminescence and energy transfer of $\text{Eu}^{2+}/\text{Mn}^{2+}$ in $\text{Ca}_2\text{PO}_4\text{Cl}$, a series of $\text{Ca}_2\text{PO}_4\text{Cl}:\text{Eu}^{2+}, \text{Mn}^{2+}$ samples are synthesized, and luminescent property is systematically investigated. Fig.3 shows emission spectra of $\text{Ca}_2\text{PO}_4\text{Cl}:0.07\text{Eu}^{2+}, y\text{Mn}^{2+}$ ($y=0-0.4$) under 370 nm radiation excitation. They consist of both a broad blue band and an orange-red emission band. The broad blue emission band from 400 to 525 nm which is typically attributed to $4f^65d^1 \rightarrow 4f^7$ electronic dipole allowed transition of Eu^{2+} ion. whereas the orange-red emission band from 525 to 700 nm is attributed to ${}^4\text{T}_1-{}^6\text{A}_1$ forbidden transition of Mn^{2+} . Emission intensities of Eu^{2+} are found to decrease

monotonically with increasing Mn^{2+} concentration, whereas emission intensities of Mn^{2+} reach a maximum at $y=0.4$. Moreover, in order to study the energy transfer from Eu^{2+} to Mn^{2+} , the normalized intensities of Eu^{2+} and Mn^{2+} in $\text{Ca}_2\text{PO}_4\text{Cl}$ are recorded, and shown in the inset of Fig.3. It shows that emission intensities of Eu^{2+} decrease, and that of Mn^{2+} gradually enhance with increasing Mn^{2+} concentration. These results indicate that the efficient energy transfer of $\text{Eu}^{2+} \rightarrow \text{Mn}^{2+}$ exists in $\text{Ca}_2\text{PO}_4\text{Cl}:\text{Eu}^{2+}, \text{Mn}^{2+}$. Moreover, for the blue and orange-red emission of $\text{Ca}_2\text{PO}_4\text{Cl}:\text{Eu}^{2+}, y\text{Mn}^{2+}$, the corresponding excitation spectra are shown in Fig.4. Obviously, They have the same excitation characteristics of Eu^{2+} with different Mn^{2+} concentration, which also indicates that it involves the energy transfer from Eu^{2+} to Mn^{2+} .

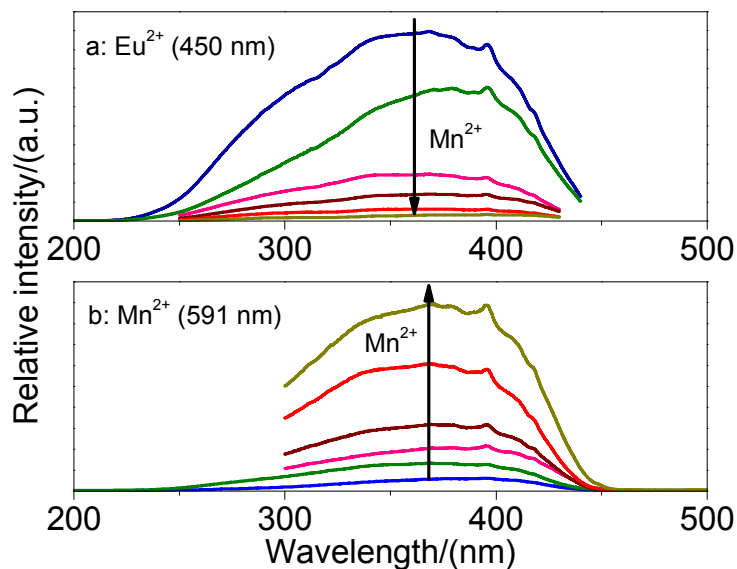


Fig.4. Excitation spectra of $\text{Ca}_2\text{PO}_4\text{Cl}:\text{Eu}^{2+}, y\text{Mn}^{2+}$ (a) ($\lambda_{\text{em}}=450$ nm) and (b) ($\lambda_{\text{em}}=591$ nm).

In order to well understand energy transfer process, energy transfer efficiency (η_T) from Eu^{2+} to Mn^{2+} of phosphors is calculated. Energy transfer efficiency (η_T) from Eu^{2+} to Mn^{2+} can be expressed according to Paulose et al.⁴⁶

$$\eta_T = 1 - (I_S/I_{S0}) \approx 1 - (\tau_S/\tau_{S0}) \quad (1)$$

where I_{S0} and I_S are luminescent intensities of sensitizer Eu^{2+} in the absence and presence of activator Mn^{2+} , and where τ_{S0} and τ_S are decay lifetimes of sensitizer Eu^{2+} in the absence and presence of activator Mn^{2+} . As shown in Fig.3, the emission intensities (I_S and I_{S0}) can be obtained, and the η_T values (the dark yellow patterns) from Eu^{2+} to Mn^{2+} for $\text{Ca}_2\text{PO}_4\text{Cl}:\text{Eu}^{2+}, y\text{Mn}^{2+}$ ($y=0-0.4$) are calculated, and are shown in Fig.5a.

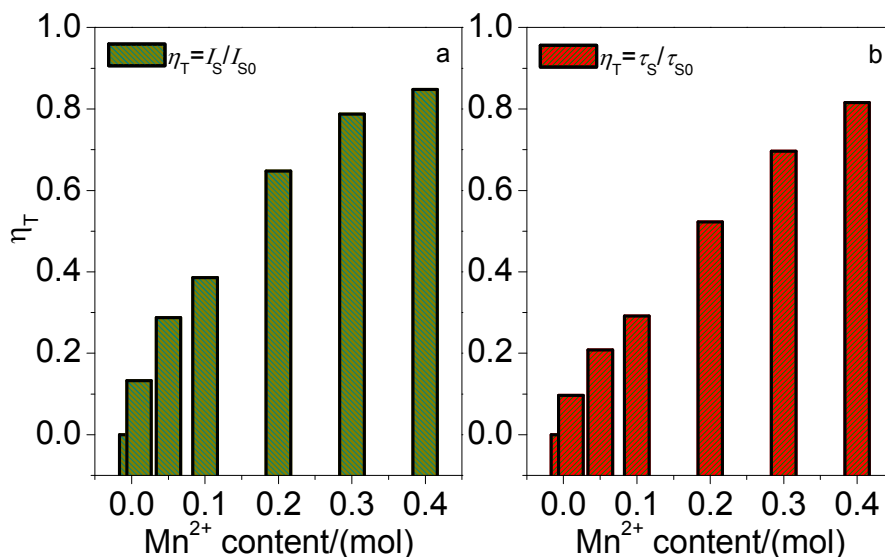


Fig.5. Variation of η_T for $\text{Ca}_2\text{PO}_4\text{Cl}:\text{Eu}^{2+}, y\text{Mn}^{2+}$ ($y=0-0.4$) with Mn^{2+} concentration.

(a): $\eta_T = 1 - (I_S / I_{S0})$; (b): $\eta_T = 1 - (\tau_S / \tau_{S0})$.

In order to achieve decay lifetimes, fluorescence lifetimes, τ , for Eu^{2+} with different Mn^{2+} concentration are measured, as a representative, Fig.6 shows the results of $\text{Ca}_2\text{PO}_4\text{Cl}:\text{Eu}^{2+}, y\text{Mn}^{2+}$ ($y=0, 0.1, 0.2$ and 0.3) ($\lambda_{\text{ex}}=375$ nm, $\lambda_{\text{em}}=450$ nm). The decay curves are well fitted with a second-order exponential decay mode by Eq.2^{11, 14, 39}

$$I = A_1 \exp(-t/\tau_1) + A_2 \exp(-t/\tau_2) \quad (2)$$

where I is luminescence intensity; A_1 and A_2 are constants; t is time, and τ_1 and τ_2 are lifetimes for rapid and slow decays, respectively. Average lifetimes (τ^*) can be obtained by using the formula as follows³²⁻³⁴

$$\tau^* = (A_1\tau_1^2 + A_2\tau_2^2) / (A_1\tau_1 + A_2\tau_2) \quad (3)$$

For $\text{Ca}_2\text{PO}_4\text{Cl}:\text{Eu}^{2+}$, $y\text{Mn}^{2+}$ ($y=0-0.4$), the calculated average lifetimes (τ^*) are 664.2, 600.0, 526.2, 470.7, 317.2, 201.9 and 122.6 ns, respectively. According to the results, energy transfer efficiency (η_T) is calculated using Eq.(1), and the η_T value can also be seen from Fig.5b (the red patterns). The results show the close proximity between using intensity and using decay time. The energy transfer efficiency from Eu^{2+} to Mn^{2+} gradually enhance with increasing Mn^{2+} concentration. At a concentration of 0.4 mol Mn^{2+} , the energy transfer efficiency is higher than 82.0%.

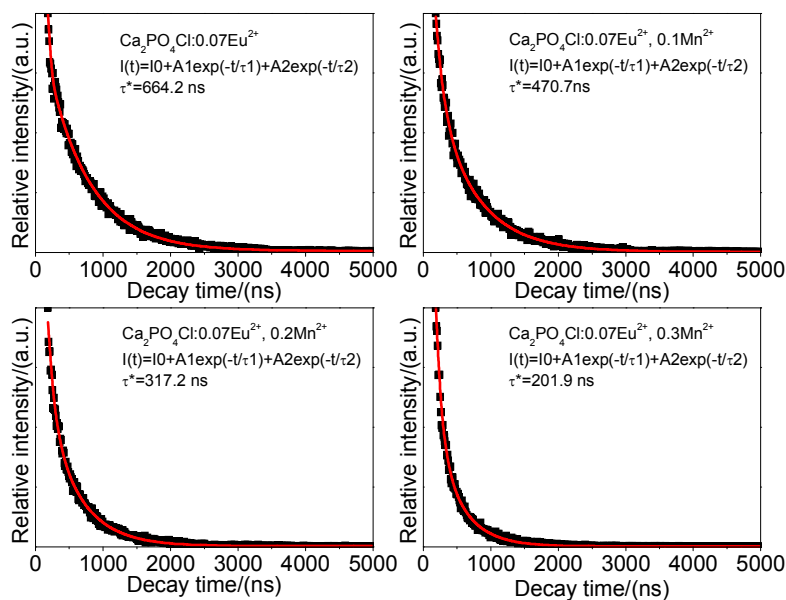


Fig.6. Decay curves of Eu^{2+} emission monitored at 450 nm for $\text{Ca}_2\text{PO}_4\text{Cl}:\text{Eu}^{2+}$, $y\text{Mn}^{2+}$ ($\lambda_{\text{ex}}=375$ nm).

On the basis of Dexter's energy transfer formula for exchange and multipolar interactions, the following relation can be obtained⁴⁷⁻⁵⁰

$$\ln(\eta_0/\eta) \propto C \quad (4)$$

$$(\eta_0/\eta) \propto C^{\omega/3} \quad (5)$$

where η_0 and η are luminescence quantum efficiency of Eu^{2+} in the absence and presence of Mn^{2+} , respectively; C is the total concentration of Eu^{2+} and Mn^{2+} . Eq.4 corresponds to exchange interaction,

and Eq.5 with $\alpha=6, 8, 10$ corresponds to dipole-dipole, dipole-quadrupole, and quadrupole-quadrupole interactions, respectively. The value of η_0/η can be approximately estimated from the correlated lifetime ratio (τ_{S0}/τ_S), so Eq.4 and 5 can be changed as follows

$$\ln(\tau_{S0}/\tau_S) \propto C \quad (6)$$

$$(\tau_{S0}/\tau_S) \propto C^{\alpha/3} \quad (7)$$

The relationships of $\ln(\tau_{S0}/\tau_S) \propto C$ and $(\tau_{S0}/\tau_S) \propto C^{\alpha/3}$ are illustrated in Fig.7. By consulting the fitting factor R , the relation $(\tau_{S0}/\tau_S) \propto C^{8/3}$ has the best fitting, implying that the dipole-quadrupole interaction is applied for the energy transfer from Eu^{2+} to Mn^{2+} .

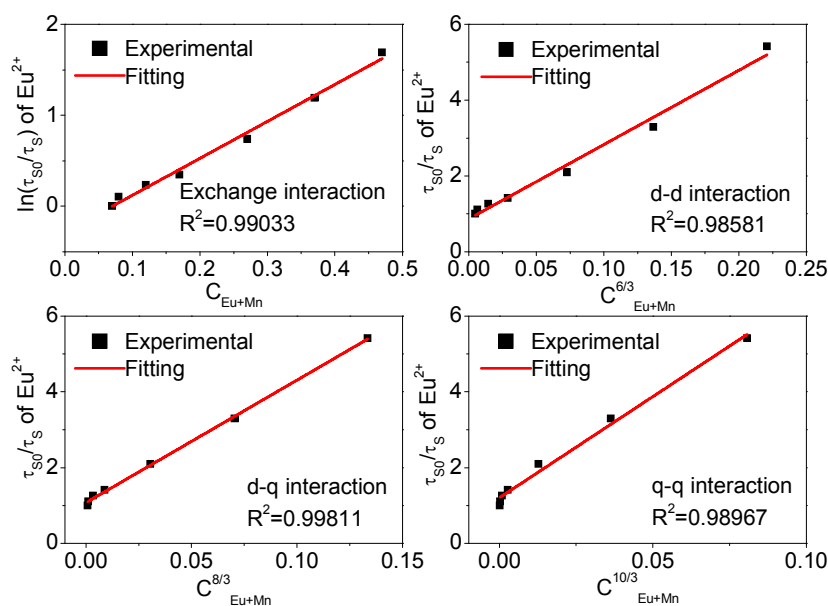


Fig.7. Dependence of $\ln(\tau_{S0}/\tau_S)$ of Eu^{2+} on (a) C and τ_{S0}/τ_S of Eu^{2+} (b) $C^{6/3}$, (c) $C^{8/3}$, and (d) $C^{10/3}$.

In general, critical distance (R_c) can be calculated using concentration quenching method. The critical distance $R_{\text{Eu-Mn}}$ between Eu^{2+} and Mn^{2+} can be estimated by⁵¹

$$R_{\text{Eu-Mn}} = 2[3V/(4\pi x_c N)]^{1/3} \quad (8)$$

where x is total concentration of Eu^{2+} and Mn^{2+} , N is number of Z ions in the unit cell (for $\text{Ca}_2\text{PO}_4\text{Cl}$, $N=4$), and V is volume of the unit cell (for $\text{Ca}_2\text{PO}_4\text{Cl}$, $V=0.46731 \text{ nm}^3$). The estimated distance

($R_{\text{Eu-Mn}}$) for $\text{Ca}_2\text{PO}_4\text{Cl}:0.07\text{Eu}^{2+}, y\text{Mn}^{2+}$ phosphors ($x_c=0.07, 0.08, 0.12, 0.17, 0.27, 0.37,$ and 0.47) are 1.47, 1.41, 1.23, 1.09, 0.94, 0.84 and 0.78 nm, respectively. The distances between Eu^{2+} and Mn^{2+} become shorter with increasing Mn^{2+} concentration. x is the critical concentration at which the emission intensity of donor (Eu^{2+}) in the presence of acceptor (Mn^{2+}) is half that in the absence of acceptor (Mn^{2+}). Therefore, the critical distance (R_c) of energy transfer is calculated to be about 1.09 nm for $\text{Ca}_2\text{PO}_4\text{Cl}:0.07\text{Eu}^{2+}, y\text{Mn}^{2+}$. $R_{\text{Eu-Mn}}$ for various Eu^{2+} content levels is much larger than the typical critical distance for exchange interaction (0.5 nm).⁵² The results indicate that the exchange interaction does not play any role in the energy transfer process for $\text{Ca}_2\text{PO}_4\text{Cl}:0.07\text{Eu}^{2+}, y\text{Mn}^{2+}$. Therefore, the emission intensities of Mn^{2+} are obviously enhanced by the efficient energy transfer from Eu^{2+} to Mn^{2+} , which belongs to the multipolar interaction.

3.4. CIE coordinates, thermal stability and quantum efficiency of $\text{Ca}_2\text{PO}_4\text{Cl}:\text{Eu}^{2+}, \text{Mn}^{2+}$

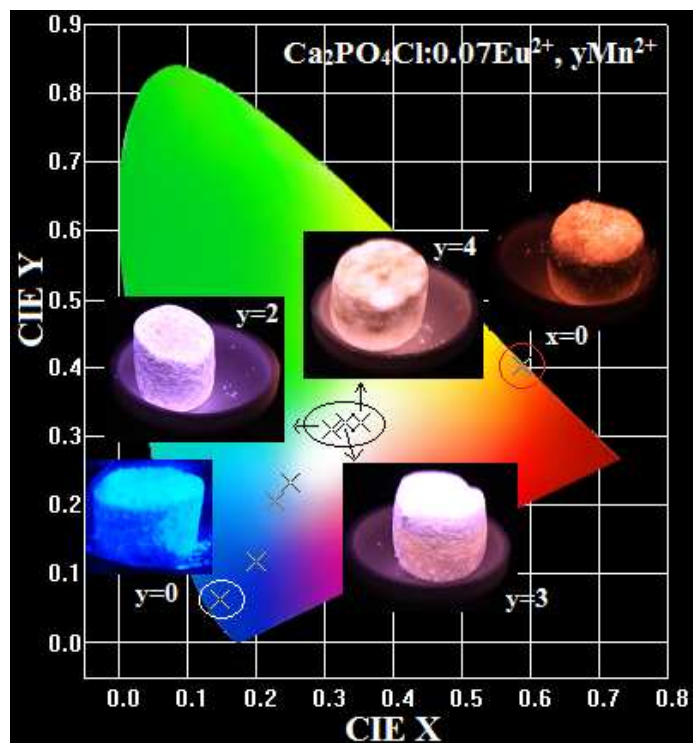


Fig. 8. CIE chromaticity coordinates and the corresponding luminescence photograph

of $\text{Ca}_2\text{PO}_4\text{Cl}:0.07\text{Eu}^{2+}, y\text{Mn}^{2+}$ ($y=0-0.4$) ($\lambda_{\text{ex}}=365$ nm).

Color coordinates are one of the important factors for evaluating the performance of phosphors. As shown in Fig.8 and Table S1, Commission Internationale de l'Eclairage (CIE 1931) chromaticity coordinates and CCT of $\text{Ca}_2\text{PO}_4\text{Cl}:0.07\text{Eu}^{2+}, y\text{Mn}^{2+}$ are measured. Eu^{2+} concentration is fixed at 0.07 as the concentration of Mn^{2+} increases from 0 to 0.4, the corresponding color of phosphor shifts from blue to white light, and eventually to orange-red. In particular, CCT of white light can also be tuned by appropriately changing Mn^{2+} concentration. It is clear that warm white light can be produced for different practical application by varying Mn^{2+} concentration in $\text{Ca}_2\text{PO}_4\text{Cl}:\text{Eu}^{2+}, \text{Mn}^{2+}$.

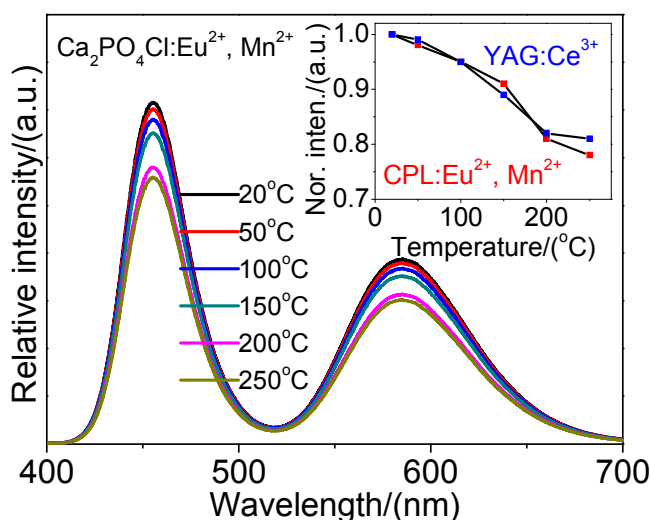


Fig.9. Temperature-dependent emission spectra of $\text{Ca}_2\text{PO}_4\text{Cl}:0.07\text{Eu}^{2+}, 0.2\text{Mn}^{2+}$ ($\lambda_{\text{ex}}=370$ nm).

Inset: normalized intensity of $\text{Ca}_2\text{PO}_4\text{Cl}:0.07\text{Eu}^{2+}, 0.2\text{Mn}^{2+}$ and $\text{YAG}:\text{Ce}$ as function of temperature.

For the application of high power LEDs, the thermal stability of phosphor is one of the important issues to be considered. For $\text{Ca}_2\text{PO}_4\text{Cl}:0.07\text{Eu}^{2+}, y\text{Mn}^{2+}$, the temperature dependence of emission spectra under 370 nm radiation excitation is shown in Fig.9. The inset depicts temperature quenching characteristics of commercial $\text{YAG}:\text{Ce}$ and typical sample $\text{Ca}_2\text{PO}_4\text{Cl}:0.07\text{Eu}^{2+}, 0.2\text{Mn}^{2+}$ in the temperature range from 20 to 250 °C. Compared with $\text{YAG}:\text{Ce}$, the emission intensity of $\text{Ca}_2\text{PO}_4\text{Cl}:0.07\text{Eu}^{2+}, 0.2\text{Mn}^{2+}$ is very close to that of $\text{YAG}:\text{Ce}$ when the temperature is raised up to

200 °C, for example, the intensity of the sample drops to about 81% when the temperature is 200 °C, while that of YAG:Ce decreases to 82% of the initial value. The results obviously indicate that the sample also has good thermal quenching properties.

For white LEDs application, quantum efficiency (QE) is an important parameter for LED phosphors. In general, a tunable white light emission with suitable QE can be obtained in $\text{Ca}_2\text{PO}_4\text{Cl}:0.07\text{Eu}^{2+}, y\text{Mn}^{2+}$ by the efficient energy transfer from Eu^{2+} to Mn^{2+} ions, as shown in Table S1. For the warm white light emitting phosphor $\text{Ca}_2\text{PO}_4\text{Cl}:0.07\text{Eu}^{2+}, 0.2\text{Mn}^{2+}$, the QE can reach 59.6%. These data indicate that $\text{Ca}_2\text{PO}_4\text{Cl}:0.07\text{Eu}^{2+}, 0.2\text{Mn}^{2+}$ has relatively appropriate QE and warm white light emission, and therefore, it could be used as phosphor for white LEDs.

3.5. Spectrum of the white LEDs fabricated with $\text{Ca}_2\text{PO}_4\text{Cl}:\text{Eu}^{2+}, \text{Mn}^{2+}$

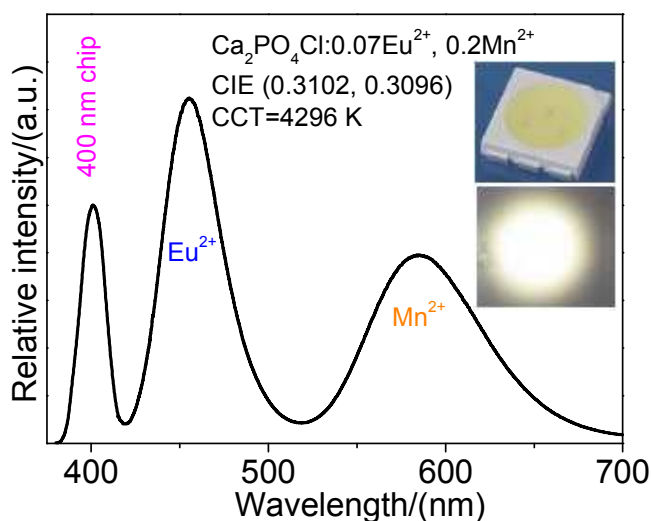


Figure 10. Emission spectrum of a pc-LED lamp fabricated with a 400 nm LED chip and warm white-emitting phosphor $\text{Ca}_2\text{PO}_4\text{Cl}:0.07\text{Eu}^{2+}, 0.2\text{Mn}^{2+}$.

Inset shows the appearance of a well-packaged trichromatic LED lamp in operation.

To demonstrate the potential application of $\text{Ca}_2\text{PO}_4\text{Cl}:\text{Eu}^{2+}, \text{Mn}^{2+}$, a white LED is fabricated by coating the $\text{Ca}_2\text{PO}_4\text{Cl}:0.07\text{Eu}^{2+}, 0.2\text{Mn}^{2+}$ phosphor on a 400 nm UV-chip that is driven by a 350 mA current. The emission spectrum of white LEDs is represented in Fig.10, which has the CIE color

coordinates (0.3102, 0.3096), the correlated color temperature (CCT) 4296K, and the color rendering index (R_a) 86, respectively. The results demonstrate that the performance of white LEDs based on $\text{Ca}_2\text{PO}_4\text{Cl}:0.07\text{Eu}^{2+}, 0.2\text{Mn}^{2+}$ phosphor is superior to white LEDs that are fabricated by coating YAG:Ce yellow phosphor on blue chips [(0.292, 0.325), CCT=7756 K] because the former shows higher color rendering index and lower CCT value.⁴

4. Conclusions

In summary, $\text{Ca}_2\text{PO}_4\text{Cl}:\text{Eu}^{2+}, \text{Mn}^{2+}$ can be excited by n-UV excitation, and the corresponding color of phosphor can shift from blue to white light, and eventually to orange-red by the efficient resonant energy transfer from Eu^{2+} to Mn^{2+} ions in $\text{Ca}_2\text{PO}_4\text{Cl}$. In particular, the warm white emission phosphor can be realized by combining emission of Eu^{2+} and Mn^{2+} in $\text{Ca}_2\text{PO}_4\text{Cl}$. The energy transfer efficiency enhances with increasing Mn^{2+} content, and the dipole-quadrupole interaction is applied for the energy transfer from Eu^{2+} to Mn^{2+} . A warm white light emitting diode is fabricated by using the warm white emitting phosphor $\text{Ca}_2\text{PO}_4\text{Cl}:0.07\text{Eu}^{2+}, 0.2\text{Mn}^{2+}$ pumped by a 400 nm LED-chip with good CIE chromaticity coordinates (0.3102, 0.3096), lower CCT (4296K) and high color rendering index (R_a) 86, respectively. Therefore, $\text{Ca}_2\text{PO}_4\text{Cl}:\text{Eu}^{2+}, \text{Mn}^{2+}$ can serve as a potential white light emitting phosphor for white LEDs.

Acknowledgments

The work is supported by the National Natural Science Foundation of China (No. 50902042), the Natural Science Foundation of Hebei Province, China (No.A2014201035; E2014201037) and the Education Office Research Foundation of Hebei Province, China (Nos.ZD2014036; QN2014085).

References

1 M. Shang, C. Li and J. Lin. Chem. Soc. Rev., 2014, 43, 1372.

- 2 C. C. Lin, R.-S. Liu. *J. Phys. Chem. Lett.*, 2011, 2, 1268.
- 3 S. Ye, F. Xiao, Y. X. Pan, Y. Y. Ma, Q. Y. Zhang. *Mater. Sci. Eng. R*, 2010, 71, 1.
- 4 C.-W. Yeh, W.-T. Chen, R.-S. Liu, S.-F. Hu, H.-S. Sheu, J.-M. Chen, H. T. Hintzen. *J. Am. Chem. Soc.*, 2012, 134, 14108.
- 5 J. Hou, W. Jiang, Y. Fang, F. Huang. *J. Mater. Chem. C*, 2013, 1, 5892.
- 6 Z. Wang, P. Li, Q. Guo, Z. Yang. *Mater. Res. Bull.*, 2014, 52, 30.
- 7 C. Zhang, S. Huang, D. Yang, X. Kang, M. Shang, C. Peng, J. Lin. *J. Mater. Chem.*, 2010, 20, 6674.
- 8 C.-H. Huang, T.-S. Chan, W.-R. Liu, D.-Y. Wang, Y.-C. Chiu, Y.-T. Yeh, T.-M. Chen. *J. Mater. Chem.*, 2012, 22, 20210.
- 9 H. Liu, Y. Luo, Z. Mao, L. Liao, Z. Xia. *J. Mater. Chem. C*, 2014, 2, 1619.
- 10 W. Lü, Z. Hao, X. Zhang, Y. Luo, X. Wang, J. Zhang. *Inorg. Chem.*, 2011, 50, 7846.
- 11 C.-H. Huang, T.-M. Chen. *J. Phys. Chem. C*, 2011, 115, 2349.
- 12 X. M. Liu, C. K. Lin, J. Lin. *Appl. Phys. Lett.*, 2007, 90, 081904.
- 13 C. C. Chang, T.-M. Chen. *Appl. Phys. Lett.*, 2007, 91, 081902.
- 14 C.-H. Huang, T.-M. Chen, W.-R. Liu, Y.-C. Chiu, Y.-T. Yeh, S.-M. Jang. *ACS Appl. Mater. Interfaces*, 2010, 2, 259.
- 15 W.-R. Liu, C.-H. Huang, C.-W. Yeh, J.-C. Tsai, Y.-C. Chiu, Y.-T. Yeh, R.-S. Liu. *Inorg. Chem.*, 2012, 51, 9636.
- 16 W.-R. Liu, C.-H. Huang, C.-W. Yeh, Y.-C. Chiu, Y.T. Yeh, R.-S. Liu. *RSC Adv.*, 2013, 3, 9023.
- 17 G. Li, Y. Zhang, D. Geng, M. Shang, C. Peng, Z. Cheng, J. Lin. *ACS Appl. Mater. Interfaces*, 2012, 4, 296.

- 18 G. Li, D. Geng, M. Shang, Y. Zhang, C. Peng, Z. Cheng, J. Lin. *J. Phys. Chem. C*, 2011, 115, 21882.
- 19 D. Geng, M. Shang, Y. Zhang, H. Lian, Z. Cheng, J. Lin. *J. Mater. Chem. C*, 2013, 1, 2345.
- 20 Y. Zhang, G. Li, D. Geng, M. Shang, C. Peng, J. Lin. *Inorg. Chem.*, 2012, 51, 11655.
- 21 N. Guo, Y. Zheng, Y. Jia, H. Qiao, H. You. *J. Phys. Chem. C*, 2012, 116, 1329.
- 22 G. Zhu, S. Xin, Y. Wen, Q. Wang, M. Que, Y. Wang. *RSC Adv.*, 2013, 3, 9311.
- 23 N. Guo, Y. Jia, W. Lü, W. Lv, Q. Zhao, M. Jiao, B. Shao, H. You. *Dalton Trans.*, 2013, 42, 5649.
- 24 W. Li, R-J. Xie, T. Zhou, L. Liu, Y. Zhu. *Dalton Trans.*, 2014, 43, 6132.
- 25 W.-T. Chen, H.-S. Sheu, R.-S. Liu, J. P. Attfield. *J. Am. Chem. Soc.*, 2012, 134, 8022.
- 26 Q. Guo, L. Liao, Z. Xia. *J. Lumin.*, 2014, 145, 65.
- 27 Z. Xia, R.-S. Liu. *J. Phys. Chem. C*, 2012, 116, 15604.
- 28 L. Huang, M. Guo, S. Zhao, D. Deng, H. Wang, Y. Hua, G. Jia, S. Xu. *ECS J. Solid State Sci. Technol.*, 2013, 2, R3083.
- 29 Z. Fu, X. Wang, Y. Yang, Z. Wu, D. Duan, X. Fu. *Dalton Trans.*, 2014, 43, 2819.
- 30 L. Ning, Y. Wang, Z. Wang, W. Jin, S. Huang, C. Duan, Y. Zhang, W. Chen, H. Liang. *J. Phys. Chem. A*, 2014, 118, 986.
- 31 S. Hu, W. Tang. *J. Lumin.*, 2014, 145, 100.
- 32 R. Yu, H. M. Noh, B. K. Moon, B. C. Choi, J. H. Jeong, K. Jang, H. S. Lee, S. S. Yi. *Mater. Res. Bull.*, 2014, 51, 361.
- 33 Z. Xia, J. Zhuang, L. Liao. *Inorg. Chem.*, 2012, 51, 7202.
- 34 Z. Xia, J. Zhuang, A. Meijerink, X. Jing. *Dalton Trans.*, 2013, 42, 6327.
- 35 J. Zhou, Z. Xia, M. Yang, K. Shen. *J. Mater. Chem.*, 2012, 22, 21935.

- 36 Z. Xia, R.-S. Liu, K.-W. Huang, V. Drozd. *J. Mater. Chem.*, 2012, 22, 15183.
- 37 Z. Xia, X. Wang, Y. Wang, L. Liao, X. Jing. *Inorg. Chem.*, 2011, 50, 10134.
- 38 M. Jiao, Y. Jia, W. Lü, W. Lv, Q. Zhao, B. Shao, H. You. *J. Mater. Chem. C*, 2014, 2, 90.
- 39 W. Lv, W. Lü, N. Guo, Y. Jia, Q. Zhao, M. Jiao, B. Shao, H. You. *Dalton Trans.*, 2013, 42, 13071.
- 40 W. Lv, W. Lü, N. Guo, Y. Jia, Q. Zhao, M. Jiao, B. Shao, H. You. *RSC Adv.*, 2013, 3, 16034.
- 41 M. Greenblatt, E. Banks, B. Post. *Acta Crystallographica*, 1967, 23, 166.
- 42 M. Greenblatt, E. Banks, B. Post. *Acta Crystallographica section B*, 1969, 25, 2170.
- 43 A. Meijering, G. Blasse. *J. Phys.: Condens. Matter*, 1990, 2, 3619.
- 44 Y.-C. Chiu, W.-W. Liu, C.-K. Chang, C.-C. Liao, Y.-T. Yeh, S.-M. Jang, T.-M. Chen. *J. Mater. Chem.*, 2010, 20, 1755.
- 45 R. Yu, C. Guo, T. Li, Y. Xu. *Curr. Appl. Phys.*, 2013, 13, 880.
- 46 P. I. Paulose, G. Jose, V. Thomas, N. V. Unnikrishnan, M. K. R. Warriar, *J. Phys. Chem. Solids*, 2003, 64, 841.
- 47 D. L. Dexter, J. H. Schulman. *J. Chem. Phys.*, 1954, 22, 1063.
- 48 R. Reisfeld, E. Greenberg, R. Velapoldi, B. Barnett, *J. Chem. Phys.*, 1972, 56, 1698.
- 49 U. Caldiño, J. L. Hernández-Pozos, C. Flores, A. Speghini, M. Bettinelli. *J. Phys.: Condens. Matter*, 2005, 17, 7297.
- 50 R. Martínez-Martínez, M. García, A. Speghini, M. Bettinelli, C. Falcony, U. Caldiño. *J. Phys.: Condens. Matter*, 2008, 20, 395205.
- 51 G. Blass, *Philips Res. Rep.*, 1969, 24, 131.
- 52 G. Blasse, B. C. Grabmaier. *Luminescent Materials*, Berlin: Springer, 1994.

